

Nematic spectral signatures of the Hund's metal

Laura Fanfarillo,^{1,2} Angelo Valli,³ and Massimo Capone¹

¹*Scuola Internazionale Superiore di Studi Avanzati (SISSA), Via Bonomea 265, 34136 Trieste, Italy*

²*Department of Physics, University of Florida, Gainesville, Florida, USA*

³*Institute for Theoretical Physics, Vienna University of Technology, 1040 Vienna, Austria*

We show, by means of dynamical mean-field theory calculations, that the experimental fingerprints of the nematic order in iron-based superconductors are intrinsically connected with the electronic correlations in the Hund's correlated metallic state and they can not be accessed via a renormalized quasiparticle picture. In particular, our results show that: (i) in a metal in which correlations are dominated by the Hund's coupling the nematic ordering does not produce a rigid energy shift in the photoemission spectra, but a much richer spectral weight redistribution which mirrors the experimental results; (ii) the nematic ordering is characterized by an orbital-selective coherence induced by the Hund's physics in agreement with the experimental picture.

Several quantum materials display a large anisotropy in the electronic properties which has been identified as a signature of electronic nematic order where the in-plane rotational symmetry of the electron fluid is broken making x and y directions inequivalent. This appears to be an ubiquitous phenomenon in iron-based superconductors (FeSC) [1–4].

Among the different experimental probes, a crucial piece of information can be obtained by Angle-Resolved Photoemission Spectroscopy (ARPES) exploiting different polarization of light to selectively probe different iron orbitals. This is particularly relevant in light of the prominent role of the orbital degree of freedom in the electronic structure of FeSC [5]. ARPES studies reveal that the band dispersion in the nematic phase is characterized by a momentum-modulated energy splitting of the xz and yz orbitals. Early studies mainly focused on FeSe [6–9] where nematicity emerges in the absence of long-range magnetic order, but the same pattern has been recently observed in BaFe₂As₂ [10]. Recent in-depth investigations have revealed that the nematic instability does not only affect the band dispersion, but also the incoherent spectral weight redistribution [11–13] and the orbital-selective coherence of the excitations close to the Fermi energy [12, 13].

A large body of experimental evidence suggests that the origin of the nematic phase is an electronic instability inducing anisotropy in the B_{2g} channel [2, 3]. Both Ising spin-nematic models and orbital-fluctuation based approaches have been proposed and extensively discussed in the literature [1, 4]. Regardless of the origin of the nematic instability, the characterization of the nematic phase of FeSC as emerging from experiments, clearly calls for a theoretical scheme which includes the sizeable electron-electron interactions and the consequent correlation effects, which are responsible of non-trivial redistribution of spectral weight at different energy scales, as well as the presence of orbital-selective coherence in the many-body nematic state. The crucial role of electron-electron interactions does not come as a surprise after several investigations demonstrating that peculiar,

orbital-selective, correlation effects dominate the normal-state of the FeSC [14].

The identification of orbital-selective Mott physics is one of the outcomes of a theoretical path which has clarified the central role of the Hund's coupling in the multi-orbital systems [14–25]. In this framework, the normal phase has been identified as a Hund's metal, a strongly correlated bad metallic state with distinctive correlation properties [14, 15, 26–41] in which orbital-selective physics emerges as a consequence of an effective decoupling between orbitals in a high-spin state [14, 36, 40, 42].

While we have a fairly good understanding of the role of electronic correlations in the normal state, much less is known about broken-symmetry phases. The link with the nematic phase has been touched upon in [43, 44] using slave-spin mean-field theories which describe the low-energy excitations as Fermi-liquid quasiparticles. The analysis of the nematic susceptibility in the correlated regime reveals that, if the symmetry between xz and yz orbitals is explicitly broken, the nematic order is strongly affected by Hund's driven correlations that stabilize configurations with small occupation imbalance between the xz/yz orbitals [43] like e.g. the sign-change nematic order experimentally observed in FeSC [6–10].

While these slave-particle studies [43, 44] provide a reliable description of the nematic reconstruction of the band dispersion, they can not access other fundamental properties of the electronic state, such as the spectral weight transfer, which can involve different energy scales, and the coherence of the electronic states with different orbital character.

In this work we analyze the nematic spectral signatures of the Hund's metal using a theoretical description that contains the dynamical correlations of the Hund's metal, beyond the Fermi-liquid picture as treated within Dynamical Mean-Field Theory (DMFT)[45]. A similar approach has been used to show the synergy between boson-driven superconductivity and Hund's correlations thereby successfully accounting for an orbital-selective pairing [46].

Our main result is that the nematic spectral weight

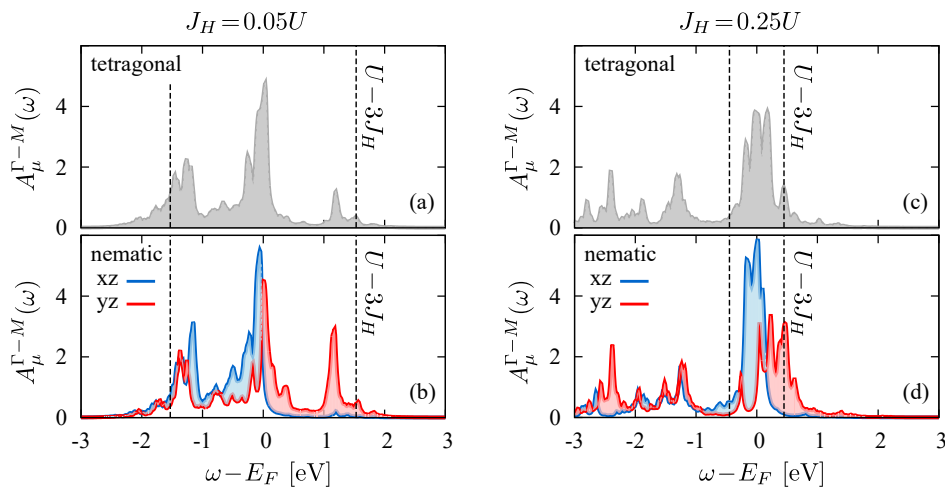


FIG. 1: Orbital spectral function in the tetragonal phase, $\eta = 0$ (a,b) and nematic phase $\eta = 50$ meV (c, d) computed using orbital and frequency-dependent DMFT self-energy for $U \sim W$ and $J_H = 0.05U$ (a,c) and $J_H = 0.25U$ (b,d). The dashed vertical lines in each panel denote the energy scale $U - 3J_H$. The nematic order introduces xz/yz orbital differentiation both in the low- and high- J_H regimes, however in the ordinary correlated metal (c) this appears as rigid shift of the xz/yz orbital slightly below/above the Fermi energy, while in the Hund's metal (d) we find an orbital-selective modulation in frequency with the xz orbital remaining closer to E_F and the yz weight moving at higher energy.

transfer in the Hund's metal is significantly different with respect to an ordinary correlated metal characterized by the similar effective mass renormalization and density of states at the Fermi level. In particular, in an ordinary correlated metal the nematic order produces a rigid energy shift of the spectral weight between the xz/yz orbitals, while the Hund's metal experiences strong orbital-selective frequency modulation of the spectra as a result of a nematic symmetry breaking.

To prove these results, we introduce a spectral nematic order parameter starting from the orbital anisotropy of the nematic spectra and show that its frequency dependence in the Hund's metal is non monotonic and controlled by multiple energy scale. This is in contrast to what happens in an ordinary correlated metal in which the characteristic energy of the nematic order dynamic is controlled by the screened Coulomb repulsion U . Our work identifies clear signatures of Hund's metal nematicity that explain the main features of the non-trivial ARPES spectra recently observed in [12, 13], thereby proving that the comprehensive experimental picture that emerges combining the observations of a reconstruction of band dispersion and the spectral weight transfer on the nematic phase of FeSC can be fully understood only accounting for the interplay of nematicity and Hund's metal physics.

In order to study the effect of electronic correlations at a reasonable computational cost we consider a minimal model, already used in [46], which accounts for the main features of the electronic structure of FeSC and for the electron-electron correlations induced by the combined effect of the Hubbard repulsion, U , and the

Hund's coupling J_H . The kinetic Hamiltonian is given by a three-orbital tight-binding model adapted from [47], $H_0 = \sum_{\mathbf{k}\sigma} \sum_{\mu\nu} T^{\mu\nu}(\mathbf{k}) c_{\mathbf{k}\mu\sigma}^\dagger c_{\mathbf{k}\nu\sigma}$ where μ, ν are orbital indices for the yz, xz, xy orbitals. $c_{\mathbf{k}\mu\sigma}^\dagger$ ($c_{\mathbf{k}\nu\sigma}$) is the fermionic operators that creates (annihilates) an electron in orbital μ , with momentum \mathbf{k} and spin σ . The set of parameters chosen (see [46]), results in a bare bandwidth $W = 1.6$ eV and reproduce qualitatively the shape and the orbital content of the Fermi surfaces typical of the FeSC family, namely two hole-like pockets composed by yz - xz orbitals at the Γ point and two elliptical electron-like pockets formed by xy and yz/xz orbitals centered at the X/Y point of the 1Fe-Brillouin Zone. Local electronic interactions are included considering the multi-orbital Kanamori Hamiltonian which parametrizes the electron-electron interactions in terms of a Hubbard-like repulsion U and an exchange coupling J_H favoring high-spin states [26].

In this work we account phenomenologically for the nematic order by adding to the Hamiltonian a bare nematic perturbation $\sim \eta(n_{yz} - n_{xz})$, $\eta > 0$. This choice, analogous to what done in [46] for the superconducting phase, reflects the aim of this paper. Rather than looking for a spontaneous nematic symmetry breaking in our simplified model, or considering a specific low-energy origin for the same instability, we focus on the role of the electronic correlations and in particular on their effect on spectral and coherence properties in the nematic phase. We compute the nematic orbital spectral functions using the full orbital and frequency-dependent DMFT self-energy $\Sigma_{\mu\mu}(i\omega_n)$, where ω_n is the n -th fermionic Matsubara frequency. In order to directly compare the outcome of our calculations with ARPES

experiments [12, 13], we integrate the orbital spectral function $A_\mu(k, \omega)$ between the high-symmetry points Γ - M of the 2Fe-Brillouin Zone. We solve DMFT using an exact diagonalization solver at zero temperature [48, 49] at a density of four electrons in three orbitals per site, that reproduces the low-energy electronic structure with hole and electron pockets including the momentum-dependence of the nematic splitting [43].

One of our main goals is to assess the effects of dynamical correlations induced by the Hund's coupling on the spectral properties in the nematic phase. The spectral functions in the tetragonal phase [16, 17, 22, 38, 46] shows indeed a qualitative effect of the Hund's coupling, which changes the typical energy scales over which the spectral weight is distributed with respect to standard correlated systems controlled by the Hubbard U .

In order to highlight these effects, we focus on two correlated regimes having similar values of $Z_\mu \sim 0.3$ in the tetragonal phase (see Table I), but characterized by different values of the Hund's coupling: $J_H = 0.05U$, $U \sim W$ define an ordinary correlated metal, while for $J_H = 0.25U$, $U \sim W$ for our occupation of four electrons in three orbitals, we are inside the Hund's metal regime. The spectra in the tetragonal state for both cases are shown in Fig. 1(a,b).

	Tetragonal	Nematic
$J_H = 0.05U$	$Z_{xz/yz} = 0.38$	$Z_{xz} = 0.45, Z_{yz} = 0.18$
$J_H = 0.25U$	$Z_{xz/yz} = 0.25$	$Z_{xz} = 0.35, Z_{yz} = 0.18$

TABLE I: Quasiparticle renormalization factors extracted by orbital-dependent DMFT self-energy. Starting from degenerate values of $Z_{xz/yz}$ in the tetragonal phase, orbital differentiation develops in the nematic state with the xz orbital remaining more coherent than the yz .

For small J_H/U we recover the familiar Mott-like behavior where Hubbard bands develop on an energy scale which approaches U in the strong-coupling limit. For larger J_H/U we find that the spectral weight reshuffling involves also a significantly smaller energy scale $\simeq U - 3J_H$, which emerges as the effective charge-charge repulsion in the Kanamori model [39].

In what follows we show that the Hund's metal state is affected by the nematic ordering in a much more subtle way with respect to the low- J_H/U regime. To some extent, the main difference with respect to an ordinary correlated metal is that the low-energy scale where the quasiparticles live is not decoupled from the high-energy ($\sim U$) features that evolve into the Hubbard bands. In the Hund's metal the spectral weight redistribution due to local interactions accumulates also in a narrower energy window around the Fermi energy [16, 17, 22, 38, 46]. This feature emerged already as crucial to boost boson-mediated superconductivity in

Hund's metal [46] and it is expected to critically affect the interplay between local electronic interactions and other low-energy instabilities including the nematic order.

In Fig. 1(c, d) we show the nematic orbital spectra for our two choices of parameters: $J_H = 0.05U$ (ordinary correlated metal) and $J_H = 0.25U$ (Hund's metal). In both regimes, the nematic order does not alter the overall energy window in which the spectral weight is distributed with respect to the tetragonal phase, however it produces a differentiation in the xz/yz orbital coherence. This can be seen both by checking the quasiparticle renormalization factors extracted from the DMFT self-energy, $Z_\mu = (1 - \partial \Im \Sigma_{\mu\mu} / \partial \omega_n)^{-1}$ listed in Table I, and by looking at the xz/yz orbital spectral weight shift towards lower/higher frequency with respect the Fermi energy in Fig. 1(c, d).

The nematic orbital transfer appears quite different in the two correlated regimes. Despite having similar quasiparticle factors Z_μ , Table I, the nematic spectra present clear signatures of Mott's or Hund's induced correlations depending of the value of J_H . In the ordinary correlated metal, panel (c), the xz/yz orbitals are almost rigidly and symmetrically shifted with respect to the tetragonal phase. In the Hund's metal instead, panel (d), the orbital shift is not symmetric and thus the orbital anisotropy of the spectra is much more pronounced. The xz spectral weight remains closer to E_F than the yz (see larger xz peak close to E_F in panel d). The yz orbital weight is transferred, instead, to much higher energies where the Hubbard bands are located. The orbital selectivity of the nematic xz/yz spectral weight transfer appears, then, a clear signature of Hund's induced correlations. This result is due to the dynamic properties of the Hund's metal. In fact, a simple differentiation of the quasiparticle renormalization factors $Z_{xz/yz}$ only accounts for a rigid shift of the xz/yz orbital spectral weight around E_F , while it cannot reproduce the orbital selective frequency dependent modulation of the nematic spectra that we observe in the Hund's metal regime.

To better visualize the frequency dependence of the orbital anisotropy of the spectral weight shown in Fig.1, we perform a frequency integration over the occupied states of the spectral function on a window of amplitude Ω

$$A_\mu(\Omega) = \int_{-\Omega}^{\Omega} d\omega \int_{\Gamma}^M dk A_\mu(k, \omega) f(\omega) \quad (1)$$

where $f(\omega)$ is the Fermi-function. The anisotropy of the xz/yz spectral function $A_\mu(\Omega)$ in the nematic phase can be analyzed by defining $\phi(\Omega) = A_{xz}(\Omega) - A_{yz}(\Omega)$. $\phi(\Omega)$ plays the role of a frequency-dependent nematic order parameter and recovers the static order parameter in the large Ω limit. In Fig.2 we show $A_{xz,yz}(\Omega)$ and $\phi(\Omega)$ for the low- and high- J_H/U regimes. In the ordinary corre-

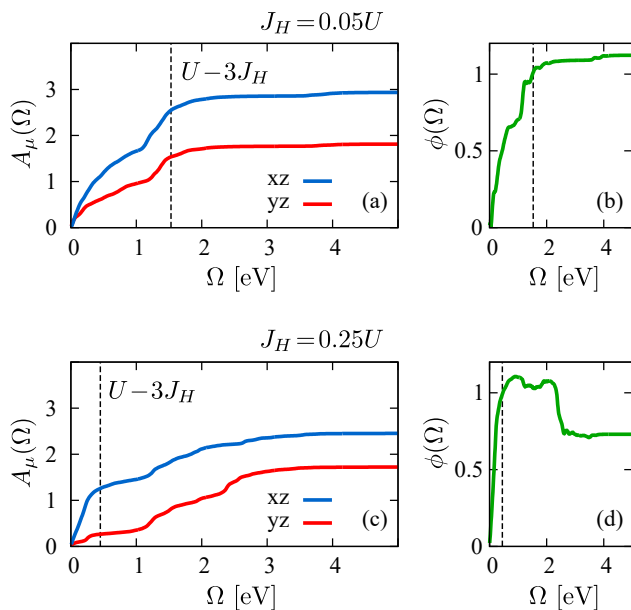


FIG. 2: (a,c) Frequency integration of the orbital nematic spectra A_μ as a function of the cut-off Ω for $U \sim W$ and $J_H = 0.05U$ (a), $J_H = 0.25U$ (c). (b,d) Frequency dependence of the nematic order parameter $\phi = A_{xz} - A_{yz}$ for the same set of parameters. The dashed vertical lines in each panel denote the energy scale $U - 3J_H$. The nematic order parameter grows monotonically up to energy $\Omega \sim U$ in the low- J_H regime. In the Hund's metal instead the nematic order grows rapidly at low frequency reaching its maximum $\Omega \sim U - J_H$, at higher energy of order U is suppressed and saturate to a constant value at higher energy.

lated metal the anisotropy of the $A_{xz/yz}$ spectral functions, panel (a), and, as a consequence, the nematic order parameter ϕ , panel (b), grow monotonically at an essentially constant rate as we increase the integration window Ω until it reaches values of order U . On the other hand, in the Hund's metal the orbital spectral function $A_{xz/yz}$, panel (c) rapidly deviate from each other for small values of Ω , but they even get closer at higher energy due to the orbital frequency modulation visible in Fig. 1. As a consequence, the energy dependence of ϕ , shown in panel (d), is characterized by a fast growth at low energy, while at frequency $\Omega > U - 3J_H$ the nematic order decreases as a function of Ω and saturate around $\Omega \sim U$ to a value approximately ~ 0.75 of the maximum.

By comparing our theoretical findings to the recent ARPES results on the orbital coherence in the nematic phase of FeSC [12, 13] we argue that the experimental spectra show clear signatures of Hund's metal nematicity characterized by an orbital-selective spectral weight redistribution qualitatively compatible with Fig.1(d) and a frequency-modulated nematic order with an intermediate-energy contribution which partially cancels the low-energy signal as shown in Fig.2(d). Moreover, our minimal model is also able to capture the experimental sign of the anisotropy of

the orbital coherence [12, 13]. Our analysis shows, in fact, that for $\eta > 0$ the xz orbital remains substantially more coherent than the yz . This is found both in the orbital-dependent static and dynamic properties of the correlated electrons, respectively encoded in the quasiparticle renormalization factor, $Z_{xz} - Z_{yz} > 0$, and the nematic frequency dependent order parameter, $\phi(\Omega) = A_{xz}(\Omega) - A_{yz}(\Omega) > 0$.

In conclusion we have analyzed the effects of electronic correlations including the Hund's exchange coupling on the nematic phase of a multiorbital model for iron-based superconductors. Comparing results for small values of the Hund's coupling, which behave as a standard Mott-Hubbard system, with large values of J_H , that drive the system into a Hund's metal, we are able to demonstrate that the effects of strong correlations on the nematic order can not be describes merely in terms of an orbital-dependent quasiparticle weight reflecting the differentiation between the xz and yz orbitals. Rather, the full frequency dependence of the interaction effects must be taken into account.

Our analysis allows us to clearly identify the distinctive signatures of the nematic spectra of a Hund's metal characterized by a frequency dependence of the nematic order and a strong differentiation of the orbital coherence. In particular we find that the nematic order parameter is dominated by a low-energy contribution, while the contribution of higher energy scales reduces the same order parameter.

Our results are in excellent agreement with experimental ARPES spectra that show how the nematic reconstruction of band dispersion is accompanied by a non-trivial spectral-weight transfer. The ability of our results to reproduce the complex experimental picture strongly supports the physical picture where the broken-symmetry phases observed in iron-based superconductors and other Hund's correlated metals can only be understood in terms of instabilities of the Hund's metal and a successful theory of these phenomena should include the dynamical correlation effects characteristic of the Hund's metal.

ACKNOWLEDGEMENTS

We are grateful to H. Pfau for helpful discussions. L. F. acknowledges financial support from the European Union Horizon 2020 research and innovation programme under the Marie Skłodowska-Curie grant SuperCoop (Grant No 838526). A. V. acknowledges financial support from the Austrian Science Fund (FWF) through through project P 31631. M.C. acknowledges financial support from MIUR through the PRIN 2017 (Prot. 20172H2SC4 005) programs and Horizon 2020 through the ERC project FIRSTORM (Grant Agreement 692670).

-
- [1] R. M. Fernandes, A. V. Chubukov, and J. Schmalian, *Nature Physics* **10**, 97 (2014), URL <https://doi.org/10.1038/nphys2877>.
- [2] A. E. Bohmer and C. Meingast, *Comptes Rendus Physique* **17**, 90 (2016), iron-based superconductors / Supraconducteurs á base de fer, URL <https://www.sciencedirect.com/science/article/pii/S1631070515001279>.
- [3] Y. Gallais and I. Paul, *Comptes Rendus Physique* **17**, 113 (2016), iron-based superconductors / Supraconducteurs á base de fer, URL <https://www.sciencedirect.com/science/article/pii/S1631070515001681>.
- [4] R. M. Fernandes, A. I. Coldea, H. Ding, I. R. Fisher, P. J. Hirschfeld, and G. Kotliar, *Nature* **601**, 35 (2022), URL <https://doi.org/10.1038/s41586-021-04073-2>.
- [5] M. Yi, Y. Zhang, Z.-X. Shen, and D. Lu, *npj Quantum Materials* **2**, 57 (2017), URL <https://doi.org/10.1038/s41535-017-0059-y>.
- [6] Y. Suzuki, T. Shimojima, T. Sonobe, A. Nakamura, M. Sakano, H. Tsuji, J. Omachi, K. Yoshioka, M. Kuwata-Gonokami, T. Watashige, et al., *Phys. Rev. B* **92**, 205117 (2015), URL <https://link.aps.org/doi/10.1103/PhysRevB.92.205117>.
- [7] L. Fanfarillo, J. Mansart, P. Toulemonde, H. Cercellier, P. Le Fèvre, F. m. c. Bertran, B. Valenzuela, L. Benfatto, and V. Brouet, *Phys. Rev. B* **94**, 155138 (2016), URL <https://link.aps.org/doi/10.1103/PhysRevB.94.155138>.
- [8] Y. Zhang, M. Yi, Z.-K. Liu, W. Li, J. J. Lee, R. G. Moore, M. Hashimoto, M. Nakaajima, H. Eisaki, S.-K. Mo, et al., *Phys. Rev. B* **94**, 115153 (2016), URL <https://link.aps.org/doi/10.1103/PhysRevB.94.115153>.
- [9] M. Yi, H. Pfau, Y. Zhang, Y. He, H. Wu, T. Chen, Z. R. Ye, M. Hashimoto, R. Yu, Q. Si, et al., *Phys. Rev. X* **9**, 041049 (2019), URL <https://link.aps.org/doi/10.1103/PhysRevX.9.041049>.
- [10] H. Pfau, S. D. Chen, M. Yi, M. Hashimoto, C. R. Rotundu, J. C. Palmstrom, T. Chen, P.-C. Dai, J. Straquadine, A. Hristov, et al., *Phys. Rev. Lett.* **123**, 066402 (2019), URL <https://link.aps.org/doi/10.1103/PhysRevLett.123.066402>.
- [11] C. Cai, T. T. Han, Z. G. Wang, L. Chen, Y. D. Wang, Z. M. Xin, M. W. Ma, Y. Li, and Y. Zhang, *Chinese Physics B* **29**, 077401 (2020), URL <https://doi.org/10.1088/1674-1056/ab90ec>.
- [12] H. Pfau, S. D. Chen, M. Hashimoto, N. Gauthier, C. R. Rotundu, J. C. Palmstrom, I. R. Fisher, S.-K. Mo, Z.-X. Shen, and D. Lu, *Phys. Rev. B* **103**, 165136 (2021), URL <https://link.aps.org/doi/10.1103/PhysRevB.103.165136>.
- [13] H. Pfau, M. Yi, M. Hashimoto, T. Chen, P.-C. Dai, Z.-X. Shen, S.-K. Mo, and D. Lu, *Phys. Rev. B* **104**, L241101 (2021), URL <https://link.aps.org/doi/10.1103/PhysRevB.104.L241101>.
- [14] L. de' Medici, G. Giovannetti, and M. Capone, *Phys. Rev. Lett.* **112**, 177001 (2014).
- [15] Z. P. Yin, K. Haule, and G. Kotliar, *Nature Materials* **10**, 932 (2011), URL <https://doi.org/10.1038/nmat3120>.
- [16] L. de' Medici, *Phys. Rev. B* **83**, 205112 (2011), URL <https://link.aps.org/doi/10.1103/PhysRevB.83.205112>.
- [17] P. Werner, M. Casula, T. Miyake, F. Aryasetiawan, A. J. Millis, and S. Biermann, *Nature Physics* **8**, 331 (2012).
- [18] F. Hardy, A. E. Böhmer, D. Aoki, P. Burger, T. Wolf, P. Schweiss, R. Heid, P. Adelman, Y. X. Yao, G. Kotliar, et al., *Phys. Rev. Lett.* **111**, 027002 (2013), URL <http://link.aps.org/doi/10.1103/PhysRevLett.111.027002>.
- [19] J. Maletz, V. B. Zabolotnyy, D. V. Evtushinsky, S. Thirupathaiiah, A. U. B. Wolter, L. Harnagea, A. N. Yaresko, A. N. Vasiliev, D. A. Chareev, A. E. Böhmer, et al., *Phys. Rev. B* **89**, 220506 (2014), URL <http://link.aps.org/doi/10.1103/PhysRevB.89.220506>.
- [20] M. Yi, Z.-K. Liu, Y. Zhang, R. Yu, J.-X. Zhu, J. Lee, F. Moore, R.G. and Schmitt, W. Li, S. Riggs, J.-H. Chu, et al., *Nat. Comm* **6**, 7777 (2015).
- [21] D. E. McNally, S. Zellman, Z. P. Yin, K. W. Post, H. He, K. Hao, G. Kotliar, D. Basov, C. C. Homes, and M. C. Aronson, *Phys. Rev. B* **92**, 115142 (2015), URL <https://link.aps.org/doi/10.1103/PhysRevB.92.115142>.
- [22] S. Backes, H. O. Jeschke, and R. Valentí, *Phys. Rev. B* **92**, 195128 (2015), URL <https://link.aps.org/doi/10.1103/PhysRevB.92.195128>.
- [23] F. Hardy, A. E. Böhmer, L. de' Medici, M. Capone, G. Giovannetti, R. Eder, L. Wang, M. He, T. Wolf, P. Schweiss, et al., *Phys. Rev. B* **94**, 205113 (2016), URL <https://link.aps.org/doi/10.1103/PhysRevB.94.205113>.
- [24] S. Lafuerza, H. Gretarsson, F. Hardy, T. Wolf, C. Meingast, G. Giovannetti, M. Capone, A. S. Sefat, Y.-J. Kim, P. Glatzel, et al., *Phys. Rev. B* **96**, 045133 (2017), URL <https://link.aps.org/doi/10.1103/PhysRevB.96.045133>.
- [25] M. D. Watson, S. Backes, A. A. Haghighirad, M. Hoesch, T. K. Kim, A. I. Coldea, and R. Valentí, *Phys. Rev. B* **95**, 081106 (2017), URL <https://link.aps.org/doi/10.1103/PhysRevB.95.081106>.
- [26] A. Georges and J. de' Medici, L. and Mravlje, *Annual Review of Condensed Matter Physics* **4**, 137 (2013).
- [27] P. Werner, E. Gull, M. Troyer, and A. Millis, *Phys. Rev. Lett.* **101**, 166405 (2008), URL <http://link.aps.org/doi/10.1103/PhysRevLett.101.166405>.
- [28] K. Haule and G. Kotliar, *New Jour. Phys.* **11**, 025021 (2009), URL <http://iopscience.iop.org/1367-2630/11/2/025021?fromSearchPage=true>.
- [29] L. de' Medici, S. R. Hassan, M. Capone, and X. Dai, *Phys. Rev. Lett.* **102**, 126401 (2009), URL <http://link.aps.org/doi/10.1103/PhysRevLett.102.126401>.
- [30] H. Ishida and A. Liebsch, *Phys. Rev. B* **81**, 054513 (2010), URL <https://link.aps.org/doi/10.1103/PhysRevB.81.054513>.
- [31] A. Liebsch and H. Ishida, *Phys. Rev. B* **82**, 155106 (2010), URL <http://link.aps.org/doi/10.1103/PhysRevB.82.155106>.
- [32] L. de' Medici, J. Mravlje, and A. Georges, *Phys. Rev. Lett.* **107**, 256401 (2011), URL <http://link.aps.org/doi/10.1103/PhysRevLett.107.256401>.
- [33] R. Yu and Q. Si, *Phys. Rev. B* **86**, 085104 (2012), URL <https://link.aps.org/doi/10.1103/PhysRevB.86.085104>.
- [34] E. Bascones, B. Valenzuela, and M. Calderón, *Phys. Rev. B* **86**, 174508 (2012), URL <http://link.aps.org/doi/10.1103/PhysRevB.86.174508>.
- [35] N. Lanatà, H. Strand, G. Giovannetti, B. Hellising, L. de' Medici, and M. Capone, *Phys. Rev. B* **87**, 045122 (2013), URL <http://link.aps.org/doi/10.1103/PhysRevB.87.045122>.

- 1103/PhysRevB.87.045122.
- [36] L. Fanfarillo and E. Bascones, Phys. Rev. B **92**, 075136 (2015), URL <http://link.aps.org/doi/10.1103/PhysRevB.92.075136>.
- [37] L. de' Medici, Weak and Strong Correlations in Fe Superconductors (Springer International Publishing, Cham, 2015), ISBN 978-3-319-11254-1.
- [38] K. Stadler, G. Kotliar, A. Weichselbaum, and J. von Delft, Annals of Physics **405**, 365 (2019), ISSN 0003-4916, URL <http://www.sciencedirect.com/science/article/pii/S0003491618302793>.
- [39] A. Isidori, M. Berović, L. Fanfarillo, L. de' Medici, M. Fabrizio, and M. Capone, Phys. Rev. Lett. **122**, 186401 (2019), URL <https://link.aps.org/doi/10.1103/PhysRevLett.122.186401>.
- [40] A. Mezio and R. H. McKenzie, Phys. Rev. B **100**, 205134 (2019), URL <https://link.aps.org/doi/10.1103/PhysRevB.100.205134>.
- [41] A. Richaud, M. Ferraretto, and M. Capone, Phys. Rev. B **103**, 205132 (2021), URL <https://link.aps.org/doi/10.1103/PhysRevB.103.205132>.
- [42] M. Capone, Nature Materials (2018), URL <https://doi.org/10.1038/s41563-018-0173-7>.
- [43] L. Fanfarillo, G. Giovannetti, M. Capone, and E. Bascones, Phys. Rev. B **95**, 144511 (2017).
- [44] R. Yu, J.-X. Zhu, and Q. Si, Phys. Rev. Lett. **121**, 227003 (2018), URL <https://link.aps.org/doi/10.1103/PhysRevLett.121.227003>.
- [45] A. Georges, G. Kotliar, W. Krauth, and M. J. Rozenberg, Rev. Mod. Phys. **68**, 13 (1996), URL <https://link.aps.org/doi/10.1103/RevModPhys.68.13>.
- [46] L. Fanfarillo, A. Valli, and M. Capone, Phys. Rev. Lett. **125**, 177001 (2020), URL <https://link.aps.org/doi/10.1103/PhysRevLett.125.177001>.
- [47] M. Daghofer, A. Nicholson, A. Moreo, and E. Dagotto, Phys. Rev. B **81**, 014511 (2010).
- [48] M. Capone, L. de' Medici, and A. Georges, Phys. Rev. B **76**, 245116 (2007), URL <https://link.aps.org/doi/10.1103/PhysRevB.76.245116>.
- [49] C. Weber, A. Amaricci, M. Capone, and P. B. Littlewood, Phys. Rev. B **86**, 115136 (2012), URL <https://link.aps.org/doi/10.1103/PhysRevB.86.115136>.